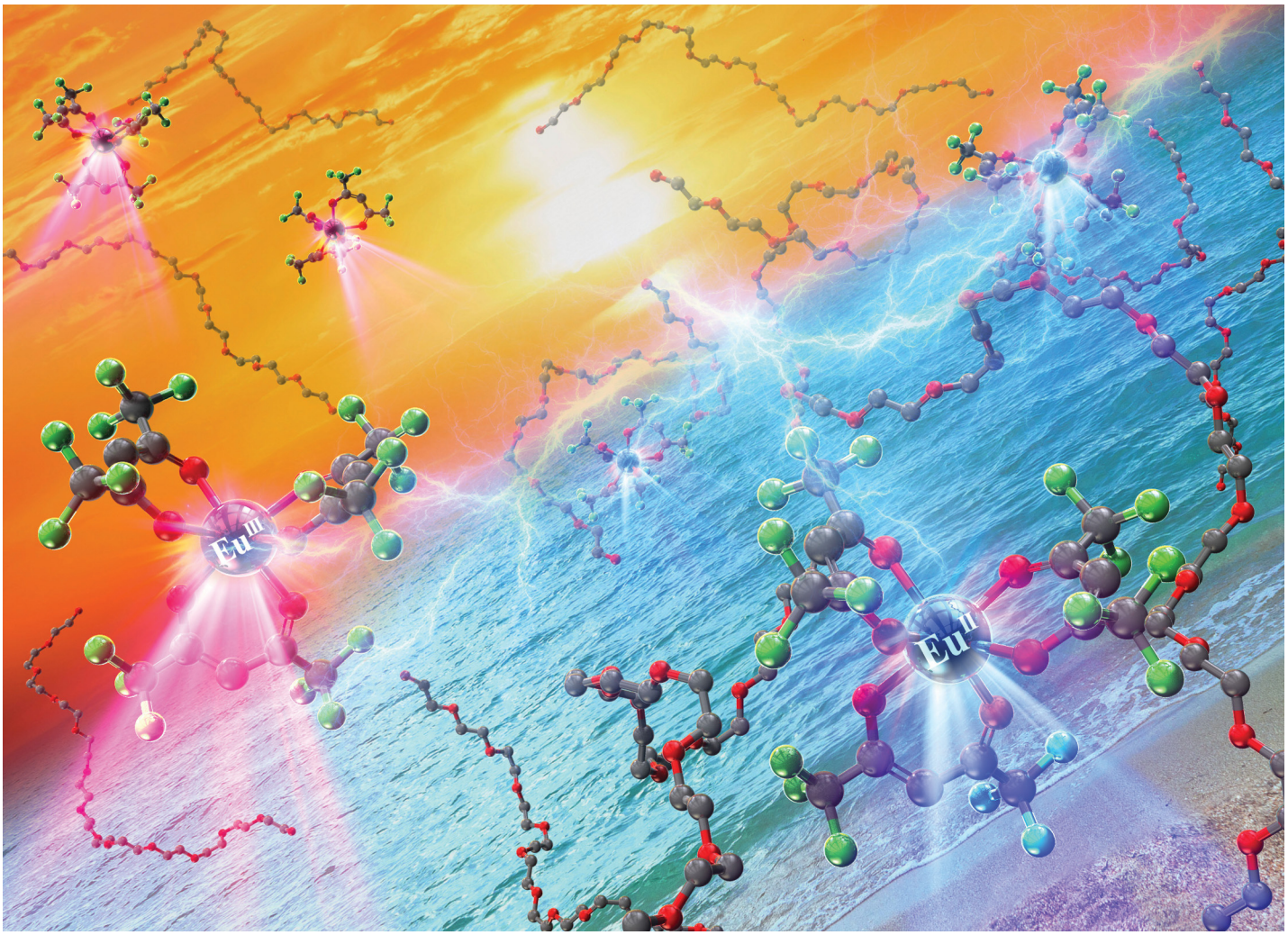

Showcasing research from the Group of Prof. Norihisa Kobayashi and Prof. Kazuki Nakamura at the Graduate School of Engineering, Chiba University.

Electrochemically regulated luminescence of europium complexes with β-diketone in polyether matrices

This study investigates the electrochemical modulation of photoluminescence colour, *i.e.* electrofluorochromism, of a europium complex in a polyether solvent. The sharp red luminescence originating from the f–f transition of Eu^{3+} was changed to broad blue luminescence from the d–f transition of the Eu^{2+} state by electrochemical redox reactions.

As featured in:

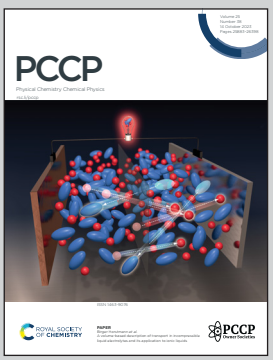

See Kazuki Nakamura *et al.*, *Phys. Chem. Chem. Phys.*, 2023, **25**, 25979.

ROYAL SOCIETY OF CHEMISTRY

rsc.li/pccp

Registered charity number: 207890

PCCP Owner Societies

PCCP

PAPER

View Article Online
View Journal | View Issue

Cite this: *Phys. Chem. Chem. Phys.*, 2023, **25**, 25979

Electrochemically regulated luminescence of europium complexes with β-diketone in polyether matrices†

Ryoto Yabuta, Norihisa Kobayashi and Kazuki Nakamura *

Received 19th May 2023,
Accepted 22nd July 2023

DOI: 10.1039/d3cp02283h

rsc.li/pccp

This study investigates the electrochemical modulation of luminescence color, *i.e.*, electrofluorochromism, of an Eu complex in a polyether solvent. The electrofluorochromic (EFC) reaction of the Eu complex occurred *via* a reversible redox reaction between Eu^{3+} and Eu^{2+}. Initially, the intrinsically stable Eu^{3+} complex showed intense red photoluminescence (PL) induced by f–f transitions. After the electrochemical reduction of Eu^{3+} to Eu^{2+}, broad blue PL was observed attributed to the d–f transitions in the Eu^{2+} complex. This distinct blue luminescence from the Eu^{2+} complex was attributed to the effective stabilization of the Eu^{2+} state by the polyether solvent. The dynamic EFC reaction that changes the valence state of the Eu ion can be potentially applied to novel chemical sensors, security devices, and display devices.

Introduction

Chromogenic materials exhibit optical properties including luminescence and absorption that can be altered using external stimuli such as light, heat, and electricity. They show potential applications in chemical sensors,[1,2] biochemical labels,[3] molecular memory,[4] and display devices.[5,6] Electrofluorochromic (EFC) materials display a change in luminescence color regulated *via* electrochemical redox reactions. They are innovative materials as they can convert electrical inputs into visual signals rapidly and repeatedly,[4,7–10] and include molecules,[11–15] conjugated polymers,[16–20] inorganic compounds,[21,22] and metal complexes.[23–29]

Ln(III) complexes are composed of a luminescent core of Ln(III) ions surrounded by antenna ligands possessing a light-absorbing capability. The luminescence of Ln(III) complexes is enhanced *via* efficient intramolecular energy transfer from the antenna ligands to the Ln(III) center, resulting in brilliant luminescence.[30–33] Furthermore, Ln(III) complexes show attractive photoluminescence (PL) properties such as characteristic and narrow emission bands in the visible-near infrared (vis-NIR) region attributed to Ln(III), long emission lifetimes, and high transparency in the visible region due to the large pseudo-Stokes shift.[34] In particular, Eu complexes have excellent emission properties, and the stabilities of their trivalent (Eu^{3+}) and divalent (Eu^{2+}) states are higher than those of other Ln(III) complexes. Eu^{3+} is characterized by intense and long-lived red luminescence induced by f–f transitions and is extensively utilized in the development of biosensors, light-emitting materials, *etc.* Eu^{2+} is characterized by broad and blue luminescence induced by d–f transitions from the excited state of $4f_6\ 5d_1$ to the ground level state of $8S_{7/2}$ ($4f_7$),[35] and the emission from Eu^{2+} in inorganic matrices could be applied to various potential luminescent devices.[36–39] The reversible control of red luminescence from Eu^{3+} and blue luminescence from Eu^{2+} *via* electrochemical redox reactions can contribute to the development of a novel display device. However, the observation of luminescence from Eu^{2+} is challenging because it is unstable in air and commonly used solutions. Therefore, previous studies reported high temperature and extended time requirements for Eu^{2+} formation; for instance, Eu^{2+}-doped zeolite derivatives were synthesized *via* annealing of Eu-containing zeolites in a reducing atmosphere at 800 °C for 3 h.[39] Additionally, the electrochemical control of trivalent and divalent ions is difficult, therefore, this study focuses on regulating the luminescence between Eu^{3+} and Eu^{2+} *via* electrochemical redox reactions. It is well-known that the blue luminescence of Eu^{2+} can be stabilized by polyethers, such as crown ethers and polyethylene glycols.[35,40] Upon stabilization, the Eu^{2+} state could be produced recurrently in a facile manner *via* the electrochemical reduction of Eu^{3+} in polyethylene glycol solutions. Considering the EFC reaction of Eu compounds, the β-diketonate Eu complex exhibiting superior red luminescence properties in the Eu^{3+} state was explored in the present study.

The electrochemical redox reactions of polyether solutions containing Eu ions and a β-diketonate Eu complex were investigated. The studies revealed that the electrochemically generated Eu^{2+} state was stable in both the solutions containing Eu ions and the Eu complex. A distinct change in luminescence color, *i.e.*, electrofluorochromism, was observed *via* the electrochemical reduction of the Eu complex in the two-electrode device using luminescence spectroscopy and the naked eye.

Graduate School of Engineering, Chiba University, 1-33, Yayoi-cho, Inage-ku, Chiba, 263-8522, Japan. E-mail: Nakamura.Kazuki@faculty.chiba-u.jp

† Electronic supplementary information (ESI) available. See DOI: https://doi.org/10.1039/d3cp02283h

Experimental

Materials

Europium nitrate hexahydrate ($Eu(NO_3)_3{\cdot}6H_2O$), tetra-*n*-butylammonium perchlorate (TBAP), silver nitrate ($AgNO_3$), propylene carbonate (PC), and acetonitrile (MeCN) were purchased from Kanto Chemical Industry Co., Japan. Dimethyl sulfoxide (DMSO) was purchased from Sigma Aldrich Japan. Hexafluoro acetylacetone (hfa) was procured from Tokyo Chemical Industry Co., Japan. Lithium trifluoromethanesulfonate (CF_3SO_3Li), lithium nitrate ($LiNO_3$), and polyethylene glycol 400 (PEG_{400}) were purchased from FUJIFILM Wako Pure Chemical Co., Japan. CF_3SO_3Li was used as the supporting electrolyte without further purification. Indium tin oxide (ITO) (10 Ω sq^{-1}; Yasuda, Japan) was used as an electrode after washing and ozonation.

Synthesis of the luminescent Eu(III) complex

Tris (hexafluoro acetylacetonate) europium ($Eu(hfa)_3(H_2O)_2$) was prepared according to a method previously reported in the literature.[41] Europium acetate *n*-hydrate was dissolved in deionized water at room temperature. Subsequently, 3 equiv. of the liquid hfa-H_2 was added dropwise into the solution. After stirring for 3 h, the obtained white precipitate was filtered and purified by recrystallization using methanol/water. Yield: 80%. Anal. Calcd for C15H7O8F18Eu: C, 22.48; H, 0.88%. Found: C, 21.52; H, 1.04%.

Preparation of the electrolyte solutions

The electrochemical redox behaviour of Eu ions was investigated using a Eu^{3+} solution containing $Eu(NO_3){\cdot}6H_2O$ (10 mmol L^{-1}) and $LiCF_3SO_3$ (500 mmol L^{-1}) in PEG_{400}. For comparison, two types of electrolyte solutions without Eu ions, namely $LiCF_3SO_3$ (500 mmol L^{-1}) in PEG_{400}, and $LiNO_3$ (60 mmol L^{-1}) and $LiCF_3SO_3$ (500 mmol L^{-1}) in PEG_{400}, were prepared. The electrochemical redox behaviour of the β-diketonate Eu complex was investigated using a PEG_{400} solution containing $Eu(hfa)_3(H_2O)_2$ (10 mmol L^{-1}) and $LiCF_3SO_3$ (500 mmol L^{-1}). For comparison, a solution composed of hfa (30 mmol L^{-1}) and $LiCF_3SO_3$ (500 mmol L^{-1}) in PEG_{400} was prepared. The solutions for optical measurements were purged with nitrogen gas for 20 min before each measurement.

Construction of EFC devices

A two-electrode cell was constructed with ITO glass electrodes or carbon-modified ITO electrodes (CM electrodes) using a silicon spacer (300 μm; Mitsubishi Chemical, Japan). CM electrodes were prepared according to a previously reported method.[42] Carbon paste was directly coated onto the ITO substrate *via* blade coating, and the gap between the blade and the ITO substrate was 180 μm. The obtained porous CM electrode was heated to 250 °C for 1 h on a hot plate. The Eu complex solution was sandwiched between the ITO electrodes (ITO–ITO device) or between the ITO and CM electrodes (ITO–CM device) to evaluate their electrochromic and PL properties.

Electrochemical measurements

For the electrochemical measurements, a three-electrode cell comprising an ITO electrode as the working electrode, Pt wire (φ = 1 mm) or a CM electrode as the counter electrode, and an Ag/Ag^+ electrode as the reference electrode were used. The reference electrode was prepared by injecting an Ag^+ solution (10 mmol L^{-1} $AgNO_3$ and 100 mmol L^{-1} TBAP in MeCN) into a sample holder with ion-permeable glass (BAS, Japan), and sealing with a cap containing an Ag wire (φ = 1 mm). Cyclic voltammetry (CV) measurements of the three-electrode cell were conducted using an electrochemical analyzer (ALS 440A, CH Instruments Inc., USA).

Photophysical measurements

The PL spectra of $Eu(NO_3)_3{\cdot}6H_2O$ and $Eu(hfa)_3(H_2O)_2$ in the electrolyte solution were obtained using a JASCO FP-6600 spectrofluorometer. Quartz optical cells with an optical path length of 1 cm and the three-electrode electrochemical cell were used for the measurements. For the two-electrode EFC devices, the luminescence properties were characterized using an epifluorescence unit (JASCO EFA-133). Excitation wavelengths of 272 and 365 nm were used for the $Eu(NO_3)_3{\cdot}6H_2O$ and $Eu(hfa)_3(H_2O)_2$ solutions, respectively. The excitation spectra at a detection wavelength of 450 nm were obtained by subtracting the Raman scattering of PEG_{400}.

Electrode potential measurement

Electrode potential measurements were performed to characterize the redox behavior of the $Eu(hfa)_3(H_2O)_2$ solution using two electrochemical analyzers, namely HZ-7000 (Hokuto Denko Co., Japan) and ALS 440A, as shown in Scheme 1, following the method in our previous report.[43] An ITO electrode was used as the working electrode, ITO or CM electrodes as the counter electrodes (the distance between the electrodes was 1 cm), and an Ag/Ag^+ electrode placed between the counter electrodes was used as the reference electrode.

Results and discussion

Redox and luminescence properties of Eu ions and the Eu complex in PEG_{400}

The CV curves of $Eu(NO_3)_3{\cdot}6H_2O$ in PEG_{400} using the constructed three-electrode cell structure are shown in Fig. 1,

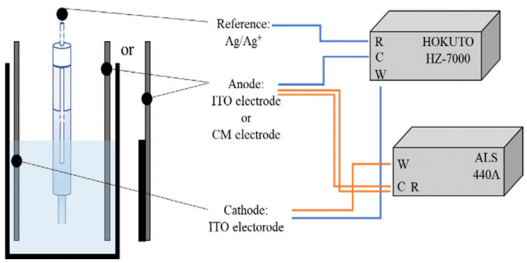

Scheme 1 The structure of a two-electrode cell system for the measurement of electrode potential using two electrochemical analyzers.

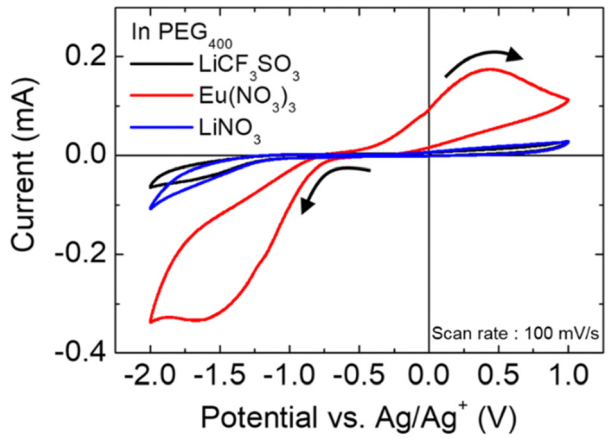

Fig. 1 Cyclic voltammograms of $Eu(NO_3)_3{\cdot}6H_2O$ or $LiNO_3$ in PEG_{400}. ($[LiCF_3SO_3]$ = 500 mM, $[Eu(NO_3)_3{\cdot}6H_2O]$ = 10 mM, $[LiNO_3]$ = 60 mM).

displaying the redox current corresponding to the reduction and oxidation reactions of Eu ions dissolved in PEG_{400}.

Scanning from the negative potential direction, a reduction current appeared from −0.75 V, reaching a maximum at −1.65 V. Scanning backward in the positive direction, an oxidation current corresponding to the reverse reaction was observed at −0.50 V. In contrast, no distinct redox current was observed for the electrolyte solution without Eu ions. Therefore, it is inferred that the redox current observed for the PEG_{400} solution containing Eu ions was due to the redox reaction of Eu^{3+}/Eu^{2+}. The ratio of the oxidation charge to the reduction charge of the Eu ion (Q_a/Q_c) in PEG_{400} was calculated to be approximately 54% whereas the ratios measured in common electrochemical solvents were relatively low (14% for DMSO, 16% for MeCN, and 13% for PC) (Fig. S1, ESI†). This indicates that the electrochemically generated Eu^{2+} is more stable in the PEG_{400} solution as compared to that in the other solvents. Fig. 2 shows the change in the emission spectrum of the $Eu(NO_3)_3{\cdot}6H_2O$ solution. When a reduction potential at −1.65 V was applied for 60 min, a new emission band was observed at approximately 430 nm.

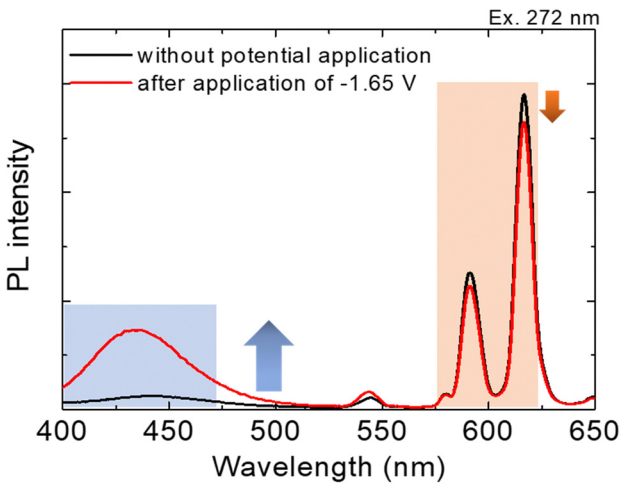

Fig. 2 Emission spectra of the $Eu(NO_3)_3{\cdot}6H_2O$ solution in a three-electrode electrochemical cell with/without an applied reduction potential (−1.65 V). Excitation wavelength = 272 nm.

It is proposed that Eu^{2+} is electrochemically generated and a broad emission band owing to the d–f transition in Eu^{2+} appeared. Simultaneously, the red emission intensity owing to f–f transitions in excited Eu^{3+} slightly decreased. Using the solvents, such as DMSO, MeCN, or PC, blue luminescence from Eu^{2+} was not observed (Fig. S2, ESI†), indicating that among all the solvents used in this study, the electrochemically generated blue luminescent Eu^{2+} is stable only in the PEG solution. However, the change in luminescence owing to both Eu^{3+} and Eu^{2+} in $Eu(NO_3)_3{\cdot}6H_2O$ was weak and could not be detected with the naked eye because the excited state of the free Eu ions without ligands undergoes luminescence quenching owing to the organic solvent. Moreover, the excitation efficiency (*i.e.*, the light absorption ability) of Eu ions was low due to the parity forbidden f–f transition.[44] To improve the luminescence intensity of the developed EFC system, an Eu complex with β-diketonate ligands was used, which exhibited strong red luminescence in organic solutions. Thus, the redox and PL properties of the β-diketonate Eu complex were determined.

Fig. 3 shows the CV curves of $Eu(hfa)_3(H_2O)_2$ in PEG_{400} using the constructed three-electrode cell. When the potential was scanned in the negative direction, a reduction current flowed from −0.85 V, and the corresponding oxidation reaction was observed when the potential was scanned back in the positive direction.

The redox reaction of $Eu(hfa)_3(H_2O)_2$ occurred at approximately the same potential as that of Eu ions in PEG_{400} as depicted in Fig. 1. Moreover, the solution containing only the hfa ligand did not exhibit a significant redox reaction in this potential range, indicating that the Eu complex exhibited the same Eu^{3+}/Eu^{2+} redox reaction as that of Eu ions in the PEG_{400} solution. Fig. 4 shows the change in the emission spectra of the $Eu(hfa)_3(H_2O)_2$ solution. When a reduction potential of −1.80 V was applied for 30 min, a broad emission band of Eu^{2+} was observed at approximately 430 nm. As the Eu^{2+} emission

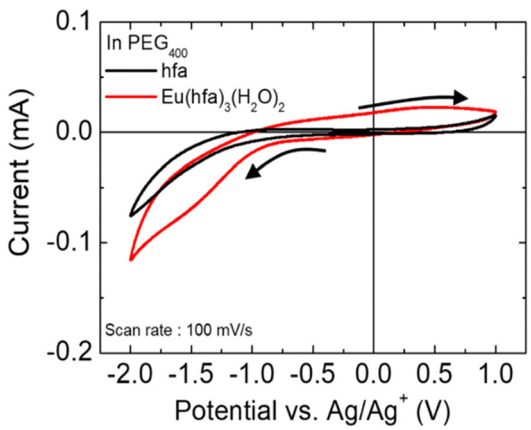

Fig. 3 Cyclic voltammograms of $Eu(hfa)_3(H_2O)_2$ or hfa in PEG_{400}. ($[LiCF_3SO_3]$ = 500 mM, $[Eu(hfa)_3(H_2O)_2]$ = 10 mM, [hfa] = 30 mM).

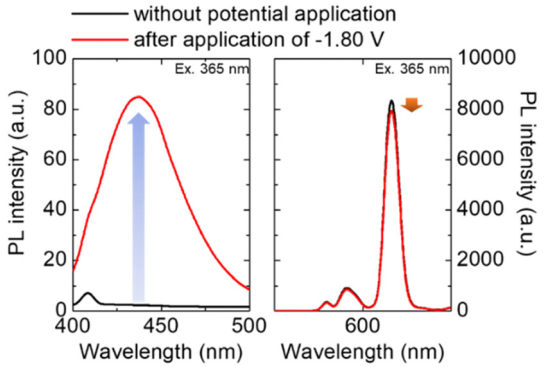

Fig. 4 Emission spectra of the $Eu(hfa)_3(H_2O)_2$ solution in a three-electrode electrochemical cell with/without an applied reduction potential (−1.80 V). Excitation wavelength = 365 nm.

increased, the red emission from Eu^{3+} at 615 nm slightly decreased, indicating that the emission shapes of the Eu complex can be electrochemically controlled between the Eu^{3+} and Eu^{2+} states for the β-diketonate Eu complex. This emission control was not observed for other solvents, such as MeCN (Fig. S3, ESI†), as depicted for Eu ions without ligands. Therefore, the Eu^{2+} state in the β-diketonate complex is stabilized in the PEG solution.

To elucidate the luminescence mechanism of the Eu complex, the excitation spectra of the $Eu(hfa)_3(H_2O)_2$ solution during the redox reaction were obtained by monitoring the Eu^{2+} emission at 450 nm and Eu^{3+} emission at 616 nm (Fig. 5).

The luminescence from the Eu^{3+} state without potential application (Fig. 5(a), black line), resulted in a large excitation band and a small band with a maximum at 365 and 396 nm being observed. The large excitation band corresponds to light absorption by the hfa ligand, and the small excitation band is attributed to the f–f transition of Eu^{3+}. Upon effective energy transfer from the ligand to the Eu ion, the light absorption of the hfa ligand enhanced the luminescence intensity of Eu^{3+} compared to that of Eu^{3+} without hfa ligands (Fig. 5(a), dotted line). When a reduction potential of −1.80 V was applied for 30 min (Fig. 5(a), red line), the intensity of the excitation band of the Eu^{3+} state was slightly decreased with decreasing Eu^{3+} emission (Fig. 4(b)). For the blue emission of the Eu^{2+} state (Fig. 5(b)), a broad excitation band with a maximum at 365 nm was observed as the reduction of Eu^{3+} proceeded. This indicates

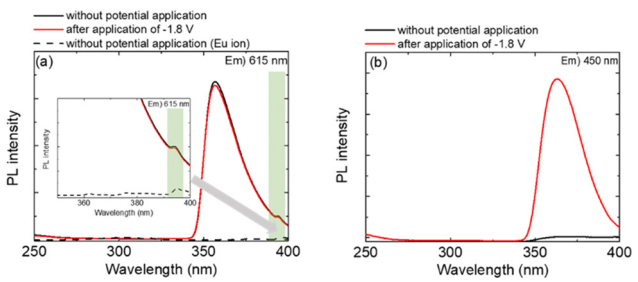

Fig. 5 Excitation spectra of the $Eu(hfa)_3(H_2O)_2$ solution before and after the application of a reduction voltage. ((a) excitation wavelength = 615 nm), (b) excitation wavelength = 450 nm).

that Eu^{2+} in $Eu(hfa)_3(H_2O)_2$ could be photo-excited *via* light absorption by the hfa ligands and subsequent energy transfer to the central Eu^{2+} ion.

However, in contrast to the increase in the Eu^{2+} luminescence intensity, a slight decrease in the Eu^{3+} luminescence intensity was observed. Eu^{2+} is generated at the electrode surface, whereas Eu^{3+} primarily occupies the solution in the cell (1 × 1 cm). To improve the contrast of the electrochemical control, two-electrode EFC devices were fabricated.

Electrofluorochromism of the Eu complex in the two-electrode devices

Fig. 6 shows the CV curves of $Eu(hfa)_3(H_2O)_2$ in PEG_{400} using the constructed two-electrode devices.

Two-electrode devices were prepared by sandwiching the Eu complex solution between two ITO electrodes (the ITO–ITO device) or between the ITO and carbon-modified ITO electrodes (ITO–CM device). When the potential is scanned in the negative direction, a redox current flowed from −2.3 and −1.5 V in the ITO–ITO and ITO–CM devices, respectively. Thus, the ITO–CM device exhibited better electrochemical properties with a lower redox voltage as compared to that of the ITO–ITO device. The difference in the redox behaviour of these two-electrode devices was investigated using electrode potential measurements. Fig. 7 shows the electrode potential (*vs.* Ag/Ag^+) measurement results for the ITO–ITO and ITO–CM devices.

The electrode potentials of the working and counter electrodes in the EFC devices (*vs.* Ag/Ag^+) were monitored during voltage scanning between the two electrodes. In both devices, the reduction current of the Eu complex flowed when the working electrode potential reached −1.0 V (*vs.* Ag/Ag^+). For the ITO–ITO device, when a voltage of −2.3 V was applied, and the working electrode potential reached −1.0 V (*vs.* Ag/Ag^+), a redox current began to flow. At this voltage, the counter electrode potential was +1.3 V (*vs.* Ag/Ag^+). Alternatively, for the ITO–CM device, when a voltage of −1.5 V was applied, the working electrode potential was −1.0 V (*vs.* Ag/Ag^+), but the counter electrode potential retained a low value of +0.5 V (*vs.* Ag/Ag^+). Using the CM

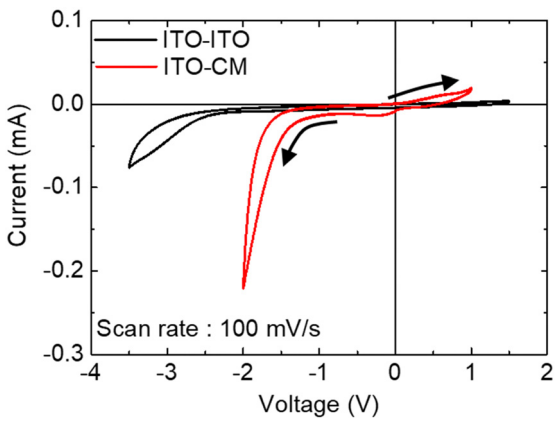

Fig. 6 Cyclic voltammograms of the $Eu(hfa)_3(H_2O)_2$ solution. (The black line represents the ITO–ITO device, and the red line represents the ITO–CM device).

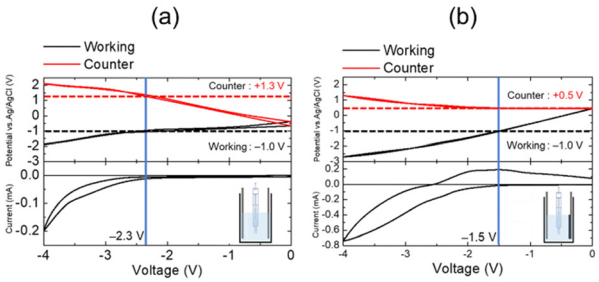

Fig. 7 Electrode potential measurement using the two-electrode devices (a) ITO–ITO and (b) ITO–CM.

electrode, a significant decrease in the driving voltage of the EFC devices was observed owing to a decrease in the reaction potential of the counter electrode from +1.3 to +0.5 V because the surface area of the CM electrode is significantly larger than that of the ITO electrode.[39] Using the CM as the counter electrode, only the working electrode potential was regulated, whereas the counter electrode potential remained the same.

Fig. 8 shows the emission spectra of the $Eu(hfa)_3(H_2O)_2$ solution in the two-electrode devices under various applied bias voltages.

When a reduction voltage was applied to the working electrode in both devices, the emission bands from the Eu^{2+} state (430 nm) increased significantly, and the red emission from the Eu^{3+} state (616 nm) decreased simultaneously as the electrochemical reduction proceeded (Fig. 8(a) and (b), red line). It is observed that the intensity ratio of Eu^{2+} emission (430 nm) to Eu^{3+} emission (616 nm) was significantly improved using the two-electrode devices; the $I_{430\ nm} : I_{616\ nm}$ ratio was 1 : 100 for the three-electrode cell and 1 : 2.5–3.0 for the two-electrode devices. Therefore, a change in the luminescence color could be detected by the naked eye after electrochemical reduction (Fig. 8 photos).

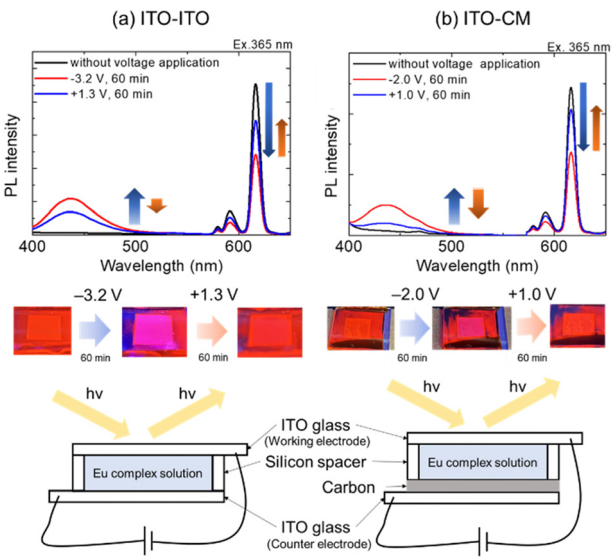

Fig. 8 Emission spectra of the $Eu(hfa)_3(H_2O)_2$ solution in PEG_{400} using a two-electrode cell ((a)ITO–ITO or (b) ITO–CM) before and after the application of reducing and oxidizing voltages.

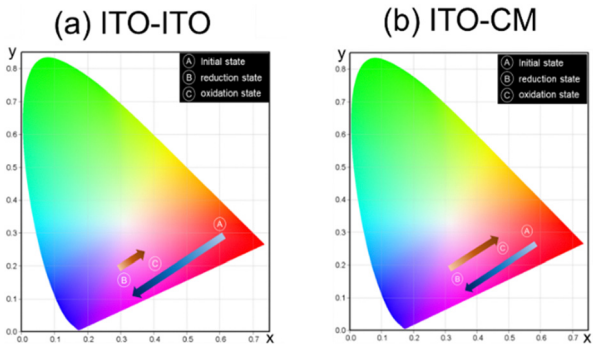

Fig. 9 The CIE chromaticity diagram of the $Eu(hfa)_3(H_2O)_2$ solution in PEG_{400} using a two-electrode cell ((a) ITO–ITO or (b) ITO–CM) before and after the application of reducing and oxidizing voltages.

Furthermore, a decrease in the degree of Eu^{3+} luminescence improves significantly for the two-electrode devices, whereas it remains unaltered in the three-electrode cell, during the electrochemical reaction.

After the oxidation of Eu ions by applying an oxidation voltage for the working electrode, the emission band from the Eu^{2+} state (430 nm) slightly decreased and the emission band from the Eu^{3+} state (615 nm) slightly increased for the ITO–ITO device (Fig. 8(a)). In contrast, the change of luminescence intensity for each band during the redox reaction of Eu ions was enhanced for the ITO–CM device (Fig. 8(b)). This result was corroborated by the CIE chromaticity diagram (Fig. 9).

Before voltage application in the initial state, both devices exhibited bright red luminescence; however, after application of the reduction voltage for the working electrode, the color hue of the luminescence changed to bluish magenta. After an oxidation voltage was applied for the working electrode, the luminescence color of the ITO–CM device was similar to its initial state, indicating good luminescence reversibility.

Conclusions

This study focused on regulating the PL color from the β-diketonate Eu complex *via* electrochemical alteration of the valence state of the Eu ions between Eu^{3+} and Eu^{2+}. The redox behaviour and changes in the luminescence properties of Eu ions and Eu complex in polyether solutions were investigated, revealing that the electrochemically generated Eu^{2+} was stable in both solutions. In the two-electrode device, a distinct change in the luminescence color *via* electrochemical reduction of the Eu complex, *i.e.*, electrofluorochromism of the Eu complex, was observed using luminescence spectroscopy and the naked eye. Initially, intense red emission from the Eu^{3+} complex was observed, and subsequently, blue emission from the Eu^{2+} complex was generated, which increased owing to the electrochemical reduction of Eu^{3+}. Furthermore, by changing the counter electrode from a flat ITO to a porous CM electrode, the reversibility of electrofluorochromism was improved due to a decreased driving voltage, which resulted in the suppression of undesired electrochemical side reactions. Therefore, this study successfully detected electrofluorochromism in the

strongly luminescent β-diketonate Eu complex for the first time. These findings could be of great significance in the development of novel display devices and chemical and biological sensors.

Author contributions

Ryoto Yabuta: investigation (Lead) and writing – original draft (Lead). Norihisa Kobayashi: writing – review & editing (Equal). Kazuki Nakamura: project administration (Lead) and writing – review & editing (Equal)

Conflicts of interest

There are no conflicts of interest to declare.

Acknowledgements

This work was partly supported by JSPS KAKENHI (17H06377, 20K05641, 22H02154, and 23K04871).

Notes and references

1 D. Tyler McQuade, A. E. Pullen and T. M. Swager, *Chem. Rev.*, 2000, **100**, 2537.
2 R. Martínez-Máñez and F. Sancenón, *Chem. Rev.*, 2003, **103**, 4419.
3 M. A. Rizzo, G. H. Springer, B. Granada and D. W. Piston, *Nat. Biotechnol.*, 2004, **22**, 445.
4 M. Irie, T. Fukaminato, T. Sasaki, N. Tamai and T. Kawai, *Nature*, 2002, **420**, 19.
5 C. Bechinger, S. Ferrere and A. Zaban, *et al.*, *Nature*, 1996, **383**, 608.
6 A. A. Argun, P. H. Aubert, B. C. Thompson, I. Schwendeman, C. L. Gaupp, J. Hwang, N. J. Pinto, D. B. Tanner, A. G. MacDiarmid and J. R. Reynolds, *Chem. Mater.*, 2004, **16**, 4401.
7 P. Audebert and F. Miomandre, *Chem. Sci.*, 2013, **4**, 575.
8 H. J. Yen and G. S. Liou, *Chem. Commun.*, 2013, **49**, 9797–9799.
9 S. Seo, S. Pascal, C. Park, K. Shin, X. Yang, O. Maury, B. D. Sarwade, C. Andraud and E. Kim, *Chem. Sci.*, 2014, **5**, 1538.
10 X. Yang, S. Seo, C. Park and E. Kim, *Macromolecules*, 2014, **47**, 7043.
11 M. Chang, W. Chen, H. Xue, D. Liang, X. Lu and G. Zhou, *J. Mater. Chem. C*, 2020, **8**, 16129.
12 M. H. Chua, Q. Zhu, K. W. Shah and J. Xu, *Polymers*, 2019, **11**, 98.
13 H. Al-Kutubi, H. R. Zafarani, L. Rassaei and K. Mathwig, *Eur. Polym. J.*, 2016, **83**, 478.
14 F. Miomandre, *Curr. Opin. Electrochem.*, 2020, **24**, 56.
15 S. Kim and Y. You, *Adv. Opt. Mater.*, 2019, **7**, 1900201.
16 K. Su, N. Sun, Z. Yan, S. Jin, X. Li, D. Wang, H. Zhou, J. Yao and C. Chen, *ACS Appl. Mater. Interfaces*, 2020, **12**, 22099.
17 C. P. Kuo, C. L. Chang, C. W. Hu, C. N. Chuang, K. C. Ho and M. K. Leung, *ACS Appl. Mater. Interfaces*, 2014, **6**, 17402.
18 J. H. Wu and G. S. Liou, *Adv. Funct. Mater.*, 2014, **24**, 6422.
19 A. Beneduci, S. Cospito, M. La Deda and G. Chidichimo, *Adv. Funct. Mater.*, 2015, **25**, 1240.
20 C. P. Kuo and M. K. Leung, *Phys. Chem. Chem. Phys.*, 2014, **16**, 79.
21 W. Gao, T. Yu, Y. Du, R. Wang, L. Wu and L. Bi, *ACS Appl. Mater. Interfaces*, 2016, **8**, 11621.
22 B. Wang, L. H. Bi and L. X. Wu, *J. Mater. Chem.*, 2011, **21**, 69.
23 Y. Kim, H. Ohmagari, A. Saso, N. Tamaoki and M. Hasegawa, *ACS Appl. Mater. Interfaces*, 2020, **12**, 46390.
24 J. Lehr, M. Tropiano, P. D. Beer, S. Faulkner and J. J. Davis, *Chem. Commun.*, 2015, **51**, 6515.
25 T. W. Ngan, C. C. Ko, N. Zhu and V. W. W. Yam, *Inorg. Chem.*, 2007, **46**, 1144.
26 F. Miomandre, R. B. Pansu, J. F. Audibert, A. Guerlin and C. R. Mayer, *Electrochem. Commun.*, 2012, **20**, 83.
27 M. Tropiano, N. L. Kilah, M. Morten, H. Rahman, J. J. Davis, P. D. Beer and S. Faulkner, *J. Am. Chem. Soc.*, 2011, **133**, 11847.
28 M. Yano, K. Matsuhira, M. Tatsumi, Y. Kashiwagi, M. Nakamoto, M. Oyama, K. Ohkubo, S. Fukuzumi, H. Misaki and H. Tsukube, *Chem. Commun.*, 2012, **48**, 4082.
29 T. Sato and M. Higuchi, *Tetrahedron Lett.*, 2019, **60**, 940.
30 J. C. G. Bünzli, *Acc. Chem. Res.*, 2006, **39**, 53.
31 J. C. G. Bünzli and C. Piguet, *Chem. Soc. Rev.*, 2005, **34**, 1048.
32 S. Faulkner, S. J. A. Pope and B. P. Burton-Pye, *Appl. Spectrosc. Rev.*, 2005, **40**, 1.
33 K. Miyata, Y. Konno, T. Nakanishi, A. Kobayashi, M. Kato, K. Fushimi and Y. Hasegawa, *Angew. Chem., Int. Ed.*, 2013, **52**, 6413.
34 A. Ishii and M. Hasegawa, *Sci. Rep.*, 2015, **5**, 11714.
35 J. Jiang, N. Higashiyama, K.-I. Machida and G.-Y. Adachi, *Coord. Chem. Rev.*, 1998, **170**, 1.
36 W. Chen, Y. Ouyang, M. Mo, H. Zhang and Q. Su, *J. Lumin.*, 2021, **229**, 117672.
37 W. Liu, L. Liu, Y. Wang, L. Chen, J. A. McLeod, L. Yang, J. Zhao, Z. Liu, J. Diwu, Z. Chai, T. E. Albrecht-Schmitt, G. Liu and S. Wang, *Chem. - Eur. J.*, 2016, **22**, 11170.
38 A. Acharjya, B. A. Corbin, E. Prasad, M. J. Allen and S. Maity, *J. Photochem. Photobiol., A*, 2022, **429**, 113892.
39 X. Yang, T. S. Tiam, X. Yu, H. V. Demir and X. W. Sun, *ACS Appl. Mater. Interfaces*, 2011, **3**, 4431.
40 M. Mukaigawa and H. Ohno, *J. Electroanal. Chem.*, 1998, **452**, 141.
41 K. Nakamura, K. Kanazawa and N. Kobayashi, *J. Photochem. Photobiol., C*, 2022, **50**, 100486.
42 Z. Liang, K. Nakamura and N. Kobayashi, *Sol. Energy Mater. Sol. Cells*, 2019, **200**, 109914.
43 R. Ozawa, K. Nakamura, T. Tachikawa and N. Kobayashi, *J. Imaging Soc. Jpn.*, 2022, **61**, 562.
44 Q. Dai, M. E. Foley, C. J. Breshike, A. Lita and G. F. Strouse, *J. Am. Chem. Soc.*, 2011, **133**, 15475.